ACS OMEGA

Open Access

http://pubs.acs.org/journal/acsodf

Article

Utilizing Food Waste in 3D-Printed PLA Formulations to Achieve Sustainable and Customizable Controlled Delivery Systems

Liwen Wang,[‖] Ling Xin Yong,[‖] and Say Chye Joachim Loo*

Cite This: *ACS Omega* 2024, 9, 34140−34150

Read Online

ACCESS | Metrics & More | Article Recommendations | Supporting Information

ABSTRACT: This is the first study that explores blending polylactic acid (PLA) with various biomasses, including food wastes—brewer's spent grain (BSG), spent coffee grounds (SCG), sesame cake (SC), and thermoplastic starch (TPS) biomass to create composite gastric floating drug delivery systems (GFDDS) through 3D printing. The aim is to investigate the influence of biomass percentage, biomass type, and printing parameters on their corresponding drug release profiles. 3D-printed (3DP) composite filaments were prepared by blending biomasses and PLA before *in vitro* drug release studies were performed using hydrophilic and hydrophobic model drugs, metoprolol tartrate (MT), and risperidone (RIS). The data revealed that release profiles were influenced by composite compositions and wall thicknesses of 3DP GFDDS capsules. Up to 15% of food waste could be blended with PLA for all food waste types tested. Delivery studies for PLA-food wastes found that MT was fully released by 4 h, exhibiting burst release profiles after a lag time of 0.5 to 1.5 h, and RIS could achieve a sustained release profile of approximately 48 h. PLA-TPS was utilized as a comparison and demonstrated variable release profiles ranging from 8 to 120 h, depending on the TPS content. The results demonstrated the potential for adjusting drug release profiles by incorporating affordable biomasses into GFDDS. This study presents a promising direction for creating delivery systems that are sustainable, customizable, and cost-effective, utilizing sustainable materials that can also be employed for agricultural, nutraceutical, personal care, and wastewater treatment applications.

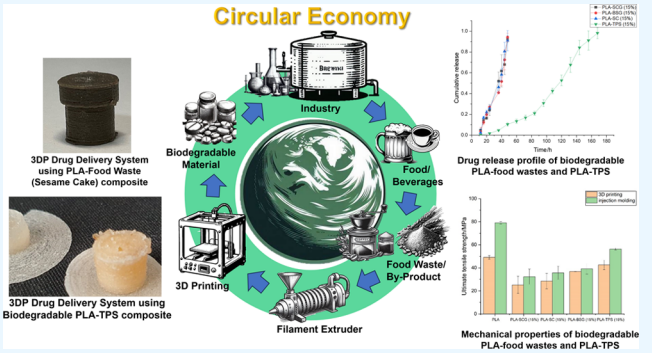

1. INTRODUCTION

Polylactic acid (PLA) is a thermoplastic polyester,[1] widely favored for its biodegradability and biocompatibility.[2,3] It is particularly suitable for biomedical applications, including achieving sustained drug release profiles as drug delivery systems. Besides biomedical-related purposes, PLA is also frequently used as a packaging material and a material ink for 3D printing.[3,4] However, the cost of PLA has been rising over the years due to increasing demand. Market analysis has forecasted that the demand for PLA would further increase to a market size of two million tonnes in 2035, from the current 350,000 tonnes.[5] With the advocate toward sustainability through a circular economy, there is, therefore, an impetus to reduce our reliance on synthetic polymers, such as PLA.

Despite the ability of PLA to degrade, its half-life ranges from 6 to 24 months.[6] On the other hand, biomasses like thermoplastic starch (TPS) and/or food wastes are sustainable material resources that offer benefits, such as shorter degradation duration. In addition, biomasses from industrial food waste are frequently disposed of in colossal quantities, often incurring additional disposal costs. Examples of industrial food waste streams include byproducts created through food production or from agricultural processes. Often these food wastes undergo incineration process which contributes to additional energy consumed, air pollution, and carbon emission.[7] Due to their homogeneity, they can actually facilitate easier valorization, particularly toward the creation of higher-value products. Homogeneous industrial food waste can therefore be processed into a sustainable source of material for blending with other synthetic materials. A composite consisting of both synthetic and biomass materials reduces the dependence on synthetic substances while preserving key attributes of the synthetic component. For instance, Filgueira et al. blended enzyme-modified thermomechanical pulp fibers with PLA and demonstrated improved water resistance of the composites.[8] Song et al. similarly reported how filament composites of good mechanical strengths can be obtained through a matrix blend of PLA with walnut shell powder.[9]

In terms of oral drug delivery applications, PLA has a degradation period that extends far beyond its pragmatic time

Received: June 1, 2024
Revised: July 4, 2024
Accepted: July 18, 2024
Published: July 26, 2024

frame. For instance, Xu et al. reported that PLA brushes have no visible degradation even after 400 h at pH 3,[10] a pH value close to that of gastric fluids. While the degradation rate of PLA is dependent on its environmental usage conditions, its manufactured form, molecular structure, and average molecular weight are factors that can influence its rate.[11,12] Drug delivery systems are typically produced by microencapsulation,[13] solvent casting,[14] hot melt extrusion,[15−17] and 3D printing process.[18] 3D printing, also known as additive manufacturing, is emerging as a popular manufacturing process as it offers advantages such as customization,[19] which is particularly advantageous for tailored or personalized drug delivery.[20] 3D printing operates as a sustainable manufacturing process that utilizes minimal material compared to subtractive manufacturing.[21] Furthermore, 3D printing can create more intricate designs and is especially beneficial for small batch or on-demand production, which allows for affordable customization of parts and products.[22] Common 3D printing processes include selective laser sintering (SLS), fused deposition modeling (FDM), and stereolithography (SLA).[23,24] The advantages of the 3D printing process and its technological progress have propelled it beyond its initial function as a mere prototype manufacturing process and have quickly transitioned into a process capable of addressing gaps unfulfilled by other manufacturing techniques.[23] The incorporation of biomass-type composites into PLA has been considered in a handful of 3D printing studies.[25,26] However, the specific use of biomass-type composites in 3DP PLA for drug delivery applications has yet to be explored.

Hence, the research gap in this study lies in the need to comprehensively assess the potential of blending food waste as biomass into PLA and using the developed composite filament to prepare 3DP gastric floating drug delivery systems (GFDDS). We aim to formulate a food waste-PLA composite through 3D printing and investigate its influence on drug release profiles. Here, we blended TPS or food wastes, brewer's spent grain (BSG), spent coffee grounds (SCG), and sesame cake (SC, also known as sesame meal waste), with PLA to understand how drug release rates can be tuned using different biomasses and compositions. Fused deposition modeling (FDM), an optimized 3D printing process, was utilized as a sustainable manufacturing technique to produce gastric floating drug delivery systems (GFDDS) using these composite materials. GFDDS enables sustained drug delivery, through the oral route, that provides a more consistent therapeutic effect. Conventionally, GFDDS were produced by using gas-generating agents and porous polymers to achieve a low-density product that can float in the stomach. However, the use of FDM allows for the development of hollow structures to achieve floatability.[27−29] This work, therefore, seeks to offer a compelling solution that yields positive environmental impacts while producing high-value products with drug delivery capabilities, at reduced material costs, through customizable 3D printing techniques.

2. MATERIALS AND METHODS

2.1. Materials. Thermoplastic starch (TPS) was prepared with corn starch (Tepung Jagung, Kon Jee Trading Co.), this was purchased from a supermarket (NTUC Fairprice Co-operative Limited). Reagent grade glycerol (Product number: G7757) was used as a plasticizer to prepare TPS, it consists of three alcohol functional groups and was presented as a colorless liquid of medium viscosity and was purchased from Sigma-Aldrich Pte Ltd. The PLA pellets, with a molecular weight (100,000 g/mol), were purchased from Natureworks 4032D. PLA has a glass transition temperature (T_g) of 63.2 °C, and a melting temperature (T_m) of 150.5 °C. The epoxidized soybean oil (ESO), used as a modifier of TPS, was purchased from Macklin Co. Ltd., China. The molecular weight of ESO is 975.40 g/mol, and the density of ESO is 0.997 g/mL. The spent coffee grounds (SCG) were provided by a Starbucks Coffee Singapore Pte Ltd. outlet. The brewer's spent grain (BSG) was obtained from Par International Pte Ltd., and the sesame cake (SC) was provided by a local factory, Oh Chin Hing Sesame Oil Factory. The model hydrophilic drug (MT) and hydrophobic drug (RIS) were purchased from Sigma-Aldrich Pte Ltd.

2.2. Preparation of Blend Materials. *2.2.1. TPS.* The corn starch was manually premixed with glycerol and water at a certain ratio based on a weight percent (%), as outlined in Table 1. The mixture was stored at ambient conditions for 24 h in a closed stainless-steel container. Subsequently, the mixture was fed into the Wellzoom desktop filament extruder purchased from Shenzhen Mistar Technology Co. Ltd., China. The rotation speed was maintained at 10 rpm, and the extruding temperature was 125 °C. The diameter of the head nozzle was 3 mm (±0.01), and the feeding velocity of the mixture was maintained at 75 g/h. TPS would be used as a biomass control for food waste.

Table 1. Raw Material Ratio for TPS Preparation

Material	Corn starch	Water	Glycerol	ESO
Weight Percent (%)	67.0	15.0	15.0	3.0

2.2.2. Preprocessing of Food Waste. Obtained BSG, SCG, and SC were sieved through a 45-mesh, and then placed in an oven of 55 °C for at least 24 h to remove moisture before blending with PLA.

2.3. Composite Filament Preparation of PLA-TPS and PLA-Food Waste (BSG, SCG, and SC). The working temperature of the Noztek Pro single extruder (Noztek, England) was set to 178 °C. The fan on the extruder was turned on throughout the extrusion process. The composite filaments were prepared using weight percentage (%). PLA-TPS and PLA-food waste filaments (composition as shown in Table 2) were dried in the oven at 55 °C for at least 12 h to remove moisture before 3D printing.

Table 2. Feedstock Ratios of PLA-Food Waste Composites and PLA-TPS Composites

Material	PLA	TPS	Food Waste
PLA-TPS (15%)	85	15	-
PLA-TPS (40%)	60	40	-
PLA-TPS (50%)	50	50	-
PLA-TPS (60%)	40	60	-
PLA-food waste (15%)	85	-	15

2.4. 3D Printing of GFDDS Capsules. Extruded filaments were printed by Ultimaker 2+ Connect (Ultimaker B.V., Netherlands) to fabricate the designed morphology. Nozzles of varying sizes were employed: 0.25, 0.4, and 0.6 mm. The prints were separated into two parts: the base cap and a top cap, printing parameter as per Table 3. The inner diameter of the bottom cap is 6.00 mm, with a printed height of 8.00 mm. The

https://doi.org/10.1021/acsomega.4c05155
ACS Omega 2024, 9, 34140−34150

top cap has an inner diameter of 6.12 mm and a height of 3.5 mm (as per Figure 1).

Table 3. FDM Printing Parameter Settings

Bed temperature (°C)	70
Shell number	1
Infill density	100%
Infill pattern	Triangles

2.5. Materials Characterization. *2.5.1. Thermal Properties.* Differential scanning calorimetry (DSC) and thermogravimetric analysis (TGA) were employed to study the melting temperature (T_m) and decomposition temperature (T_d) of both the raw materials and the composite filament. DSC measurements were performed using a TA Instruments DSC Q10 (Waters) under a nitrogen atmosphere (50 mL/min) at the temperature range of 35−220 °C and a heating rate of 5 °C/min. All DSC samples weighed between 5 and 8 mg. TGA tests were conducted using TA Instruments such as TGA Q500 (Waters). All materials were evaluated at a temperature range of 35−600 °C with a heating rate of 10 °C/min under a nitrogen atmosphere (50 mL/min). All TGA samples weighed between 4 and 6 mg.

2.5.2. Scanning Electron Microscopy (SEM). The surface morphology of the filament and 3DP GFDDS capsule was studied with a JEOL JSM-6360 scanning electron microscope (SEM) (JEOL, Japan) with an accelerating voltage of 5−15 kV. Double-sided carbon adhesive tape secured the samples to the SEM stubs. The samples were sputter-coated with gold under an argon atmosphere using an auto fine JFC 1600 coater (JEOL, Japan) prior to imaging.

2.5.3. In Vitro Drug Release Study. To test the release profile of the printed GFDDS capsule, the hydrophilic drug MT and hydrophobic drug RIS were used individually for loading into the 3DP GFDDS capsule. A shaking incubator (JEIO TECH IST-3075) was operated at 37 ± 0.5 °C with a rotation speed of 100 rpm. 20 mL of simulated gastric fluid (SGF) (99.98% 0.1 mol/L hydrochloric acid, 0.02% tween 20) was employed as the dissolution medium. An aliquot (1 mL) of the dissolution medium was withdrawn from the dissolution apparatus every 12 h and replaced with fresh medium to maintain the volume. The drug contents of the withdrawn samples were separated, recognized, and quantified by using a high-performance liquid chromatography (HPLC) technique. The withdrawn samples were filtered through a 0.20 μm nylon filter. The mobile phase for risperidone is water: acetonitrile (70:30) with 0.1% trifluoroacetic acid at 1 mL/min rate and detected at 280 nm. For MT, the same mobile phase was used at a flow rate of 1 mL/min and detected at 282 nm.

2.5.4. Mass Loss. 3DP GFDDS capsules prepared with PLA-TPS (40, 50, 60%) formulations were dried in the 50 °C oven for 24 h and put in centrifuge tubes with 20 mL of SGF after weighing and recording. Six samples were prepared for each formulation. The precipitation from the 3DP GFDDS capsules was collected at 7 and 14 days separately. Three samples were taken from tubes after 7 days and dried in the 55 °C oven for 24 h and weighed. The other three samples were taken from tubes after 14 days, dried in the 55 °C oven for 24 h, and weighed.

$$\text{mass loss \%} = (\text{weight before SGF} - \text{weight after SGF}) / \text{weight before SGF} \times 100\%$$

2.5.5. Mechanical Test. The injection molding machine (Babyplast, China) was used to prepare dumbbell-shaped specimens. PLA, PLA-TPS (15%), and PLA-food waste (15%) were chopped up into 5 mm pellets and fed through the machine hopper. The operating injection temperature is 180 °C. The injection pressure is 55 bar.

Dumbbell-shaped specimens (as shown in Figure 1) were prepared by either 3D printing or injection molding. The 3DP

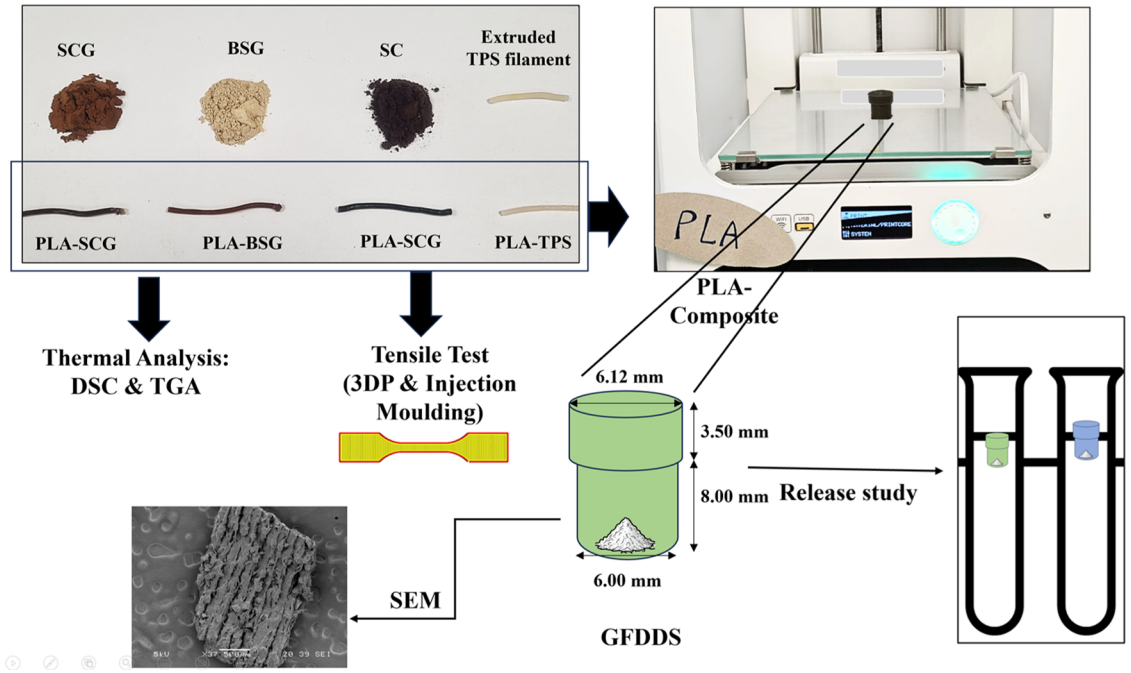

Figure 1. Schematic showing the overall process and test plan of the work. Incorporating biomass (food waste and TPS) into PLA, 3D printing the GFDDS, and finally evaluating the drug release profile of the 3DP GFDDS capsule.

https://doi.org/10.1021/acsomega.4c05155
ACS Omega 2024, 9, 34140−34150

Figure 2. (Top row, left to right) SC, BSG, SCG powder after sieving and TPS filament (second row, left to right) PLA-SC (15%), PLA-BSG (15%), PLA-SCG (15%), and PLA-TPS (15%).

specimens were built to obtain 3DP layers parallel to the shape of the dumbbell specimen. The tensile test was performed with an Instron 5567 static mechanical tester (Instron) and the measurements were carried out according to the ISO 527 standard at room temperature. The crosshead speed was set to 0.5 mm/s, and the starting force was from 0 N.

2.5.6. Statistical Analysis. For the drug release study and mechanical testing, at least three samples were tested for each group. The standard deviation and mean value of the three samples were tabulated using the data analysis software Origin 2021.

3. RESULTS AND DISCUSSION

3.1. PLA-TPS Composite Filament Preparation and Characterization. TPS and PLA-TPS composite filaments (Figure 2) were prepared by thermal extrusion at 125 and 170 °C, respectively. The temperatures were selected with reference from earlier works of A. Przybytek et al. and Haryńska et al.[30,31] The loading percentage of TPS was gradually increased from 40%, with the maximum possible loading at 60%. Further increasing the TPS percentage was found to exhibit printing challenges in the initial 3D printing trials. This difficulty is likely due to poorer mechanical performance when proportion of PLA in the composite filament is reduced (Table S1). Thermal analysis, i.e., DSC and TGA were performed to determine the influence of the TPS ratio on PLA-TPS composite (see Table S2). The weight percentages of TPS were found to influence their thermal properties. The melting point (T_m) of the PLA-TPS composites decreased from 150.5 °C (PLA) to 141.4 to 146.8 °C with the addition of TPS. Similarly, the decomposition temperature (T_d) decreased with an increasing amount of TPS, with PLA-TPS (40%) displaying a T_d of 324.5 °C, while PLA-TPS (60%) was 281.9 °C (see Table S2, TGA thermogram in Figure S2). From the DSC curve, a glass transition temperature (T_g) at about 60 °C was observed in PLA as per Figure S1(a). This T_g gradually reduces, with increasing amount of TPS in PLA-TPS as shown in Figure S1(b). An expected cold crystallization peak at around 100 °C is also present in all PLA-TPS composite filaments (DSC and TGA thermograms in Figure S1).

3.2. PLA-Food Waste Composite Filament Preparation and Characterization. The food waste was sieved prior to filament preparation so as to reduce large filler particles which may affect mechanical properties and also reduce the risk of nozzle clogging during 3D printing. The food waste needs to have low moisture content so that it does not result in filament swelling, as moisture can also lead to bubbling during the 3D printing process. The thermal properties of the various food wastes were assessed and summarized in Table 4. Melting point (T_m) and decomposition temperature (T_d) were tested by DSC and TGA, respectively. The food wastes were found with broad melting peaks (Figure S1(c)) which was expected as they are a mixture of various components with each group of food waste types. In PLA-food waste composite filaments, PLA-SCG has a significant exothermic sharp peak at 130 °C which was not observed in the other food waste composite filament (Figure S1(d)). This may be caused by thermal degradation or oxidation of certain organic compounds found in SCG.

Table 4. Melting Temperature (T_m) and Decomposition Temperature (T_d) of all Three Food Waste and PLA-Food Waste Composite Filaments Measured with DSC and TGA

Thermal Properties of Food Waste and PLA-Food Waste	BSG	SC	SCG
T_m of food waste only (°C)	103.5	140.5	135.0
T_d of food waste only (°C)	267.2	287.9	269.3
T_m of composite with 15% food waste (°C)	151.8	162.6	151.5
T_d of composite with 15% food waste (°C)	288.0	292.8	277.9

Knowledge of the thermal properties ensures that the right temperature was chosen during extrusion and 3D printing. All three food wastes possessed adequate T_d ranging from 267.2 °C − 287.9 °C to support the thermal processes required in this study. When blended as 15% composite to obtain a composite filament, the T_d value did not show a drastic difference from the T_d of food waste only (TGA thermograms of food waste and PLA-food waste in Figure S3).

Next, PLA was blended individually with three food wastes, i.e., BSG, SCG, and SC. The optimal amount of food waste and the food waste powder size that can be blended into PLA were concurrently evaluated. A midsize nozzle of 0.4 mm was selected; hence, the feedstocks were first sieved through 45-mesh to obtain powder size smaller than 0.4 mm. As per Figure 2, BSG powder which was initially a light beige color became a much darker brown filament. This darkening can be attributed to several possibilities. One possible cause is the occurrence of the Maillard reaction, a chemical reaction between amino acids and sugars that leads to the formation of brown pigments known as melanoidins and various volatile compounds.[33] The Maillard reaction has been documented in several studies involving the baking process with BSG.[34] Additionally, the presence of sugars can also lead to caramelization. Given that BSG contains various components, it is possible that some components undergo thermal degradation during filament

https://doi.org/10.1021/acsomega.4c05155
ACS Omega 2024, 9, 34140−34150

preparation at 178 °C, even though the tested T_d of BSG food waste was 255.4 °C (Table 4). Some of these reactions can also occur in SCG and SC without a visually observable change, as these food wastes were much darker than BSG.

Incorporation trials of the food waste found that an optimal percentage of 15% could be mixed with PLA without adversely affecting the filament properties, further increasing the percentage resulted in brittle filaments that were difficult to work with. This can be explained by the presence of only weak intermolecular bonds between PLA and food wastes without the addition of a binder and/or catalyst. Without strong chemical bonds, food wastes are predominantly held together by PLA and may result in weaker properties. The presence of chemical bonds also greatly depends on the chemical composition of the food wastes used. According to known literature, the main composition of SC is protein,[35] SCG is primarily composed of organic compounds such as proteins, cellulose, and lignin,[36,37] while BSG has high levels of carbohydrates.[38] There may be some weak hydrogen bonds formed from the hydroxyl groups in cellulose; however, if present, these are insufficient to significantly improve the mechanical properties.[39] Future work to perform compositional analyses of food waste will help to confirm these hypotheses. Furthermore, the diverse chemical compositions inherent in food wastes present a challenge for direct application without any modification which should be explored as well in future work.[32]

Filaments of PLA-SCG (15%), PLA-BSG (15%), and PLA-SC (15%) were also evaluated and had T_m range between 151.8 and 162.6 °C as shown in Table 4. The T_m of pure PLA measured was 150.5 °C, the incorporation of food wastes which melts at 103.5−135.0 °C had minimal influence on the T_m of the 15% composite filament. Composite filament with 15% of SC has a slightly higher T_m of 162.6 °C compared to filament with 15% BSG or 15% SCG. This is likely contributed by the SC food waste that has a higher T_m at 140.5 °C. The data obtained from the thermal study forms a foundational understanding for making adjustments to the 3D printing temperature in the subsequent stages.[30,31] Additionally, while the sieving process may help to remove larger particles there is still a possibility that food wastes fillers were not able to disperse homogeneously in the filament leading to regions with agglomeration when food waste as composite was added beyond 15%.[40] Further exploration to look at additional processes could help reduce this phenomenon when attempting to utilize a higher food waste percentage in future works.

3.3. 3D Printing Parameters for GFDDS. The GFDDS is a two-part capsule design where the top cap can fit snugly over the base cap, securing the drug within. Unlike studies that leverage the low infill percentage to produce a low-density 3DP GFDDS, the entire GFDDS was 3DP with 100% infill, and the buoyancy arises from the hollow space between the two caps.[27,41,42] To achieve stable layer-by-layer formation in FDM, the key parameters considered in this work are printing temperature, printing speed, and wall line width. Bed temperature, cooling pattern, infill density, and infill pattern were kept constant throughout the printing of all of the 3DP parts. The filament composite formulation and the respective parameters used can be found in Table 5.

Printing evaluations were carried out for the composite filament PLA-TPS (40%) and PLA-TPS (60%) with different printing nozzles. Only PLA-TPS (40%) filament could be printed with a 0.25 mm nozzle at a printing speed of 20 mm/s. Reduced nozzle diameter often necessitates a slower printing speed, as it increases the risk of clogging and filament breakage throughout the printing process. This may result in interlayer gaps in the 3DP end-product.[43] For printing with the same material using 0.4 and 0.6 mm nozzles, the larger nozzle diameters allow faster printing speed at 30 mm/s (see Table 4). Predictably, for PLA-TPS (60%) with a 0.4 mm nozzle, a lower printing speed was required for stable layer formation as the higher ratio of TPS content can reduce interlayer adhesion. When using a 0.6 mm nozzle, the wider filament provided greater interlayer contact thus improving adhesion, allowing for a faster printing speed of 30 mm/s. The wall line width (Figure 3) refers to the width of the deposited line of the material that makes up the walls of a 3DP object. For FDM, this parameter is determined by the diameter of the nozzle opening. In this design, the wall line width is also the wall thickness, which will be evaluated for its effect on the drug delivery results. As shown in Figure 3, the average wall line widths achieved were 0.27, 0.40, and 0.60 mm from 0.25 0.40, and 0.60 mm nozzles, respectively.

Table 5. Overview of FDM Printing Parameters (Printing Speed, Printing Temperature, Wall Line Width) for all Composite Filament Prepared

Parameters		Printing speed (mm/s)	Printing temperature (°C)	Wall Line Width (mm)
PLA-TPS (40%)	0.25 mm	20	174	0.18
	0.40 mm	30	178	0.35
	0.60 mm	30	178	0.50
PLA-TPS (60%)	0.40 mm	20	174	0.35
	0.60 mm	30	178	0.50
PLA-TPS (15%)	0.40 mm	30	178	0.35
PLA-BSG (15%)	0.40 mm	30	174	0.35
PLA-SC (15%)	0.40 mm	30	178	0.35
PLA-SCG (15%)	0.40 mm	30	178	0.35

The rationale behind the 3D printing parameter works similarly for composite filaments with food waste. Hence, the considerations made during the parameter adjustment for the PLA-TPS composite filament were also applied to PLA-food waste. As shown in Table 4, BSG has a T_m that is at least 30 °C lower than SC and SCG. During the 3D printing trials, PLA-SC (15%) and PLA-SCG (15%) could be well extruded at 178 °C. When evaluating the printing temperature of PLA-BSG (15%), it was observed to be much "flowier" than PLA-SC (15%) and PLA-SCG (15%) at 178 °C, which is not ideal layer-by-layer construction. Reducing the printing temperature to 175 °C allowed for appropriate flowability of PLA-BSG during 3D printing. For the filaments derived from food waste, a 0.4 mm nozzle was chosen, representing a midsized option. All food waste filaments can be printed at 30 mm/s, which is the same speed selected for PLA-TPS. No speed reduction was required to accommodate the food waste biomass component. Since the maximum amount of food waste incorporated was 15%, a sample of PLA-TPS (15%) was 3DP with the same condition using a 0.4 mm nozzle as a direct comparison to the PLA-food waste (15%).

3.4. *In Vitro* Drug Release of 3DP GFDDS. *3.4.1. PLA-TPS Capsules.* PLA degradation can last from several weeks to

https://doi.org/10.1021/acsomega.4c05155
ACS Omega 2024, 9, 34140−34150

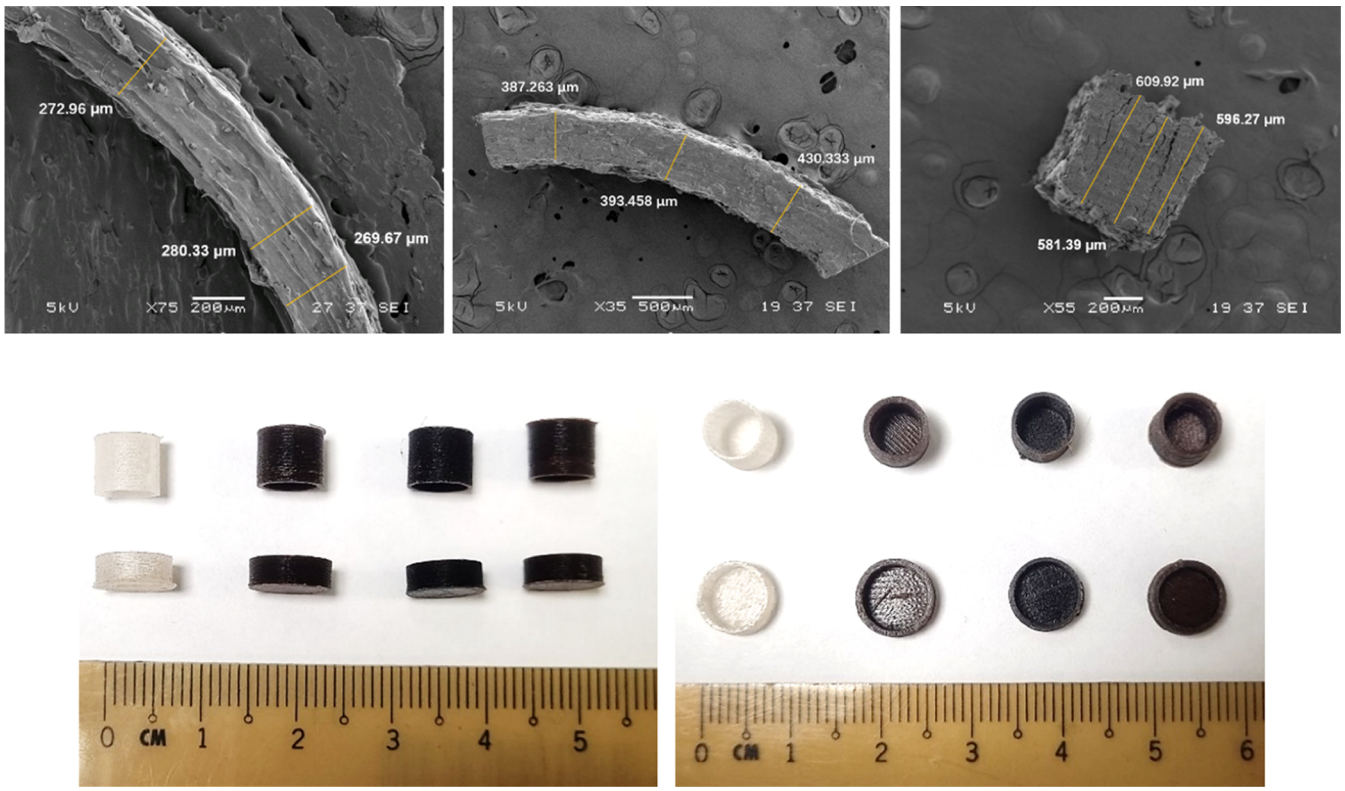

Figure 3. (Top row, left to right) PLA measurements of the wall thickness obtained with 0.25, 0.4, and 0.6 mm printing nozzle for PLA-TPS (40%). (Bottom row, left image, side view of 3DP GFDDS capsules/right image top view of 3DP GFDDS capsules with 0.4 mm wall thickness, left to right) PLA-TPS (15%), PLA-BSG (15%), PLA-SCG (15%) and PLA-SC (15%).

a year, depending on the molecular weight; this can lead to extended periods of drug release, which is not always favorable or required. Hence, different methods looking at developing PLA foam or PLA copolymer have been considered to tailor the degradation rate.[44,45] In this study specifically, we introduce the addition of hydrophilic TPS composition that will increase the degradation rate for GFDDS capsules. 3DP GFDDS PLA-TPS capsules with two different wall thicknesses (0.25 and 0.6 mm) and two different composition ratios (PLA-TPS (40%) and PLA-TPS (60%)) were prepared. The 3DP capsule showed sustained and controlled release ability for both hydrophobic RIS and hydrophilic MT. The drug release was completed between 20 and 120 h, as shown in Figure 4.

The material composition ratio of PLA-TPS and wall thicknesses were both significant factors that affect the drug release profile. In terms of PLA-TPS ratio, for the same nozzle size of 0.6 mm, a complete release of MT from PLA-TPS (60%) was observed within 33 h, while the full release in PLA-TPS (40%) required approximately 20 h (see Figure 4a). As per Figure 4c, a similar trend can be observed with RIS, the release from 3DP GFDDS capsule built with PLA-TPS (60%) was completed in about 18 h, and for PLA-TPS (40%), the complete release took 2 times longer than PLA-TPS (60%).

Visually, TPS was observed to have eluted from the PLA-TPS GFDDS capsule in SGF. As per SEM images in Figure 5b, cavities were formed and the structure of the 3DP GFDDS capsule became more porous compared to its original state prior to SGF immersion. As anticipated, formulations with a higher proportion of TPS were found to have more sediments, as indicated by a measurement of the mass loss (results in Figure S4). The formation of cavities within the 3DP capsule enhanced the permeation of the media. This mechanism elucidates how the composition ratio influences the release rate of drugs from the PLA-TPS 3DP GFDDS capsule. Similar findings have been reported in the work of other researchers. One such finding was shared by Domsta et al., the work demonstrated that reducing the polymer ratio of Eudragit RS and RL accelerated the drug release rate of 3DP implants, while a higher amount of Eudragit RS extended the release duration.[46] Moreover, in 3D printing of oral drug formulation, a common approach to modifying the drug release profile involves creating different numbers or sizes of cavities by altering infill density[47] or channels.[48]

For the wall thickness study, only PLA-TPS (40%) was selected, and a 3DP GFDDS capsule was built with 0.25 and 0.60 mm wall thicknesses. The release of both drugs was encapsulated within a 3DP GFDDS capsule with 0.60 mm wall thickness sustained for a much longer time than those prepared with 0.27 mm. In the 3DP GFDDS capsule with 0.27 mm wall thickness, up to 74% of MT was already released in the first 5 h (Figure 4b). In RIS, 0.27 mm samples released all of the drugs within 20 h, while 0.60 mm achieved sustained and controlled delivery up to 120 h. 3DP GFDDS capsule with thicker walls led to a longer pathway for SGF to penetrate the capsule, thereby lengthening the delivery time. A similar trend on the influence of wall thickness toward drug release kinetics has been reported by Maroni et. Al. The authors performed an *in vitro* test on a 3DP two-compartment device with varying shell thicknesses and found that the compartment with thicker walls exhibited a longer lag time prior to drug release.[49]

3.4.2. PLA-Food Waste Capsules. PLA-TPS (15%) was included in this test matrix as a comparison against all three PLA-food waste (15%) filaments. For MT, PLA-TPS (15%) had sustained release that was completely released by 108 h

https://doi.org/10.1021/acsomega.4c05155
ACS Omega 2024, 9, 34140−34150

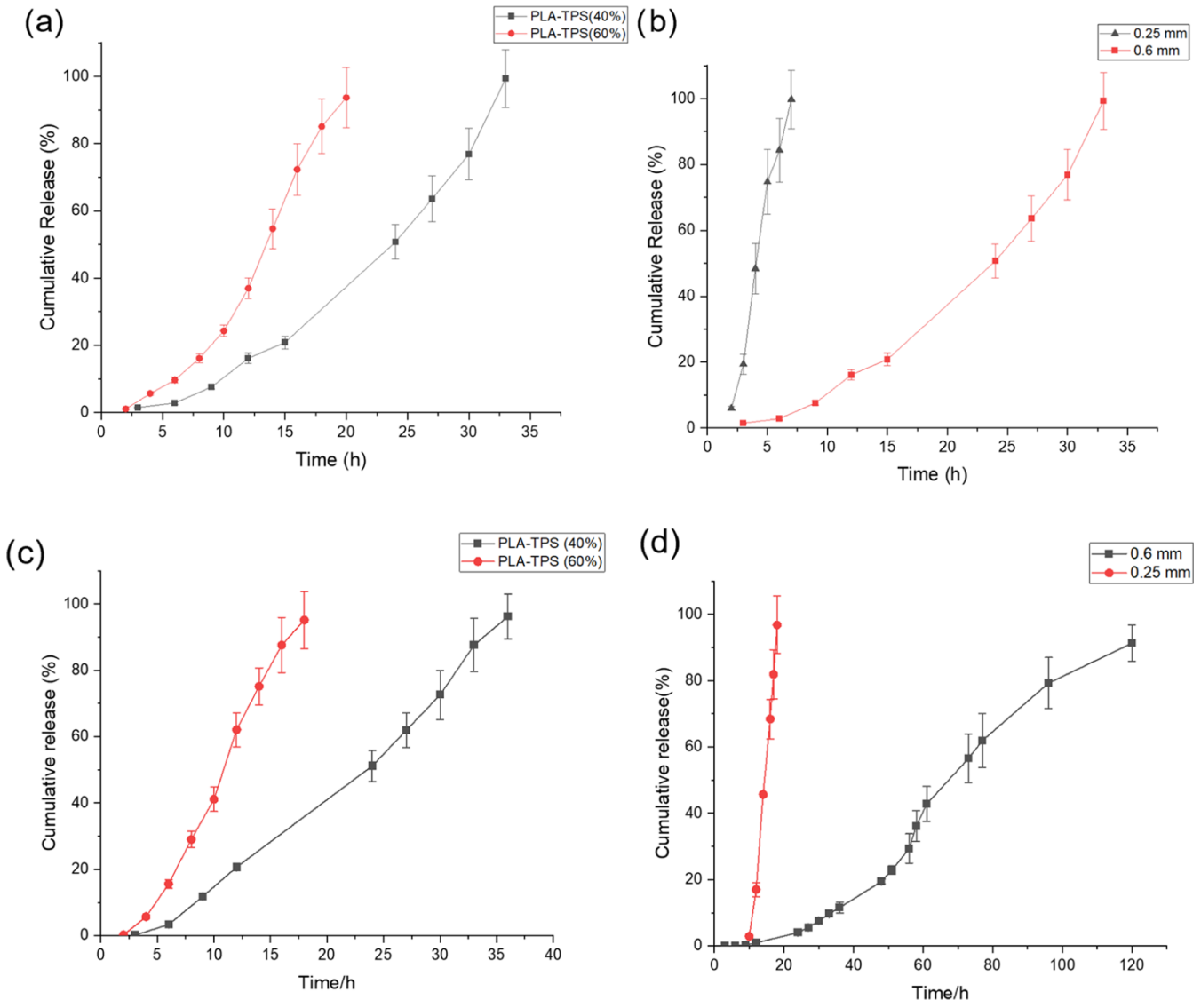

Figure 4. (a) Metoprolol Tartrate (MT) release curves of 3DP PLA-TPS (40, 60%) capsules with 0.60 mm wall thickness samples, (b) PLA-TPS (40%) for 0.25 and 0.60 mm wall thicknesses, (c) Risperidone (RIS) curves of 3DP PLA-TPS (40, 60%) capsules with 3D 0.4 mm wall thickness samples, and (d) PLA-TPS (40%) for 0.25, 0.6 mm wall thickness.

(Figure 6a). PLA-food waste (15%) demonstrated a burst release, as shown in Figure 6b. All of the drugs were released within 2 h after a lag time of 0.5−1.5 h. PLA-SC (15%) had a lag time of first 0.5 h prior to its burst release, while PLA-BSG (15%) and PLA-SCG (15%) demonstrated the burst release only toward the end of 2 h. A possible reason for the difference in the burst release time observed in PLA-SC could be due to low hygroscopicity in SC. Given that SC originates as a byproduct of sesame oil extraction, PLA-SC might retain residual oil, hindering its uptake of water, SC powder may have easily dislodged from the 3DP GFDDS capsule matrix upon contact with SGF, resulting in 1.5 h faster burst release of MT compared to PLA-BSG and PLA-SCG. Conversely, for PLA-BSG and PLA-SCG, these samples were presumed to be more hydrophilic, the food waste component may progressively swell, taking in SGF. The presence of 85% PLA in the composite restricts the swollen food waste from dislodging and releasing the drug immediately. Hence, the drug release may only be feasible after significant swelling has taken place in the food waste, leading to a buildup of pressure to expel the expanded food waste component after 2 h. Consequently, this process triggers the burst release of the MT drug from the 3DP GFDDS capsule, as observed in Figure 6b.

Such observed burst release has potential applications in conditions such as bronchial asthma, angina pectoris, and ulcers, where a rapid-release profile could offer specific benefits.[41] Furthermore, 3D printing has been demonstrated for the personalization of multidrugs within polypills[50−52] and such a burst release matrix can be used favorably; whereby some drugs can be embedded into a 3DP layer with burst release matrix to provide immediate relief of symptoms, while another 3DP layer incorporates a drug that requires sustained therapeutic effect. Alternatively, in PLA-BSG and PLA-SCG, which exhibited a delayed burst release profile after a 2 h period, this matrix may be beneficial where drug−drug interactions should be avoided.

For the RIS drug (see Figure 6c,d), all of the 3DP GFDDS capsules prepared by PLA-food waste showed sustained release with samples showing the same release trend with an initial slow release (around 20% cumulative drug release around 20

https://doi.org/10.1021/acsomega.4c05155
ACS Omega 2024, 9, 34140−34150

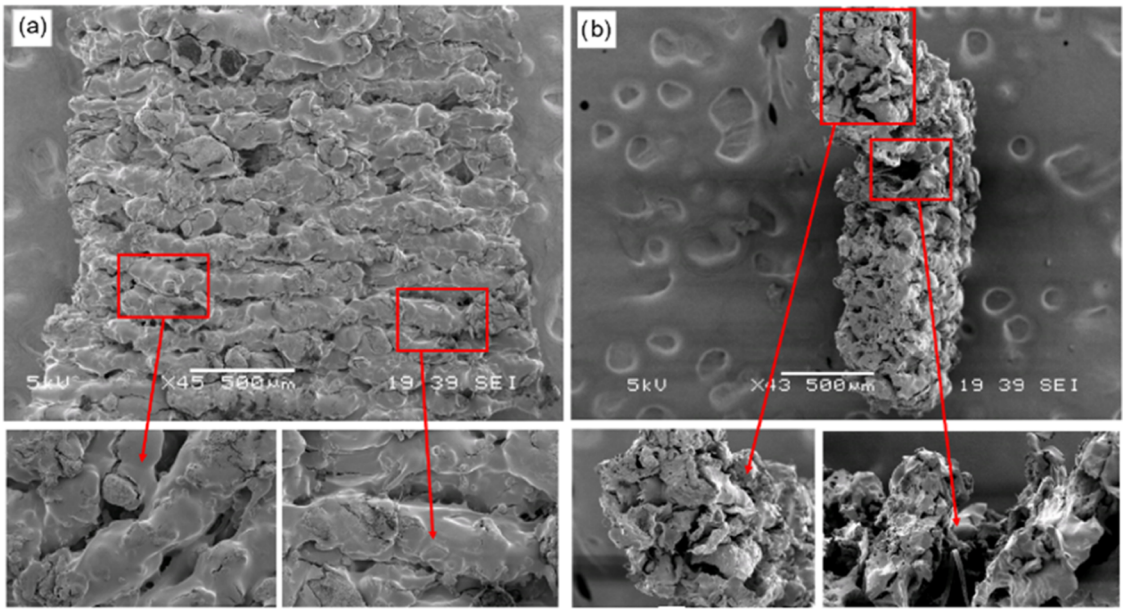

Figure 5. PLA-TPS (60%) (a) before the release study, starch granules in the 3DP GFDDS capsule were visible under SEM (b) after the release study, SEM observation of the 3DP GFDDS capsule revealed the presence of several cavities or gaps attributed to the TPS granules that had fallen out during the study.

h). The release subsequently accelerated, and the complete release of RIS was observed within 48 h. There were negligible differences between the three different food waste filaments in the release of RIS. The probable mechanism for drug release involves the penetration of water into the polymeric structures through the pores or gaps between interlayers. Given that all food waste underwent sieving through a 45-mesh, the composites' pores or gaps are expected to be uniform. With both MT and RIS drugs, 3DP GFDDS prepared with PLA-TPS (15%) had a much slower release when compared to PLA-food waste. MT was completely released after 100 h, and RIS was released after about 170 h, which is at least 3 times longer than the 3DP GFDDS capsules prepared with PLA-food waste (Figure 6c,d). For RIS, the slow initial release was also observed in the first 80 h, and the release rate increased gradually thereafter.

The SEM images (Figure 7) indicated that all of the 3DP capsules have compact structures. Additionally, some particles of food waste were visible on the surface of the filaments. Interlayer gaps similar to those observed in the 3DP PLA-TPS capsule were observed as well. There was no significant visual difference among the three 3DP PLA-food wastes—BSG, SC, and SCG.

3.5. Mechanical Properties of PLA-Food Waste. The mechanical properties of composites play a pivotal role in determining their suitability and performance across various applications. Furthermore, the weaker mechanical strength of the interlayers within 3DP parts is often compared to parts prepared with injection molding. This is a significant concern because the mechanical properties of 3D-printed objects are influenced by the print orientation and raster angle, and these properties cannot be characterized as those of a continuous material.[30,53]

In order to quickly assess the mechanical strength between the interlayers of 3DP PLA-food waste, the samples were prepared into tensile test dumbbell-shaped specimens (samples were printed at XY orientation and 90° raster angle) and compared against injection-molded samples. Expectedly, all injection-molded PLA-food waste samples have higher ultimate tensile strength than the corresponding 3DP samples (as shown in Figure 8). The compact structure produced with the injection molding process reduces voids and adhesion problems that are found within 3DP layers. While PLA has the highest tensile strength for both 3DP and injection-molded samples, there is a much bigger discrepancy between the 3DP PLA and injection-molded PLA.

The tensile strength values of PLA-food waste samples were closer between injection molding and 3DP. Among all of the PLA-food waste samples, PLA-BSG (15%) showed the smallest difference values between the 3DP and injection molding prepared ones. Among the 3DP samples incorporating biomass, 3DP PLA-TPS (15%) and PLA-BSG (15%) showed tensile strength of 42.6 MPa and 36.8 MPa, respectively. These values were the closest to the pure PLA tensile strength of 49.0 MPa, indicating a promising potential for serving as a replacement for pure 3DP PLA. Since no additives were used in the preparation of these samples, future studies to consider inclusion of additives or functionalizing/modification of the food waste to yield better compatibility between PLA and food waste would potentially lead to improved mechanical properties.

4. CONCLUSIONS

In this work, a novel approach to utilize biomass such as TPS and food wastes to tune drug release rates was achieved using PLA as a base synthetic material. TPS loading of up to 60% was attainable, whereas only 15% loading can be achieved using food waste (BSG, SCG, and SC) as filament becomes brittle when loading goes beyond 15%. PLA-food waste and PLA-TPS filaments showed comparable printability and were suitable for 3D printing via FDM, and were subsequently prepared into 3DP GFDDS capsules, containing RIS and MT, two model drugs that were individually placed in each GFDDS capsule. PLA-TPS had a variable release rate that could be

https://doi.org/10.1021/acsomega.4c05155
ACS Omega 2024, 9, 34140−34150

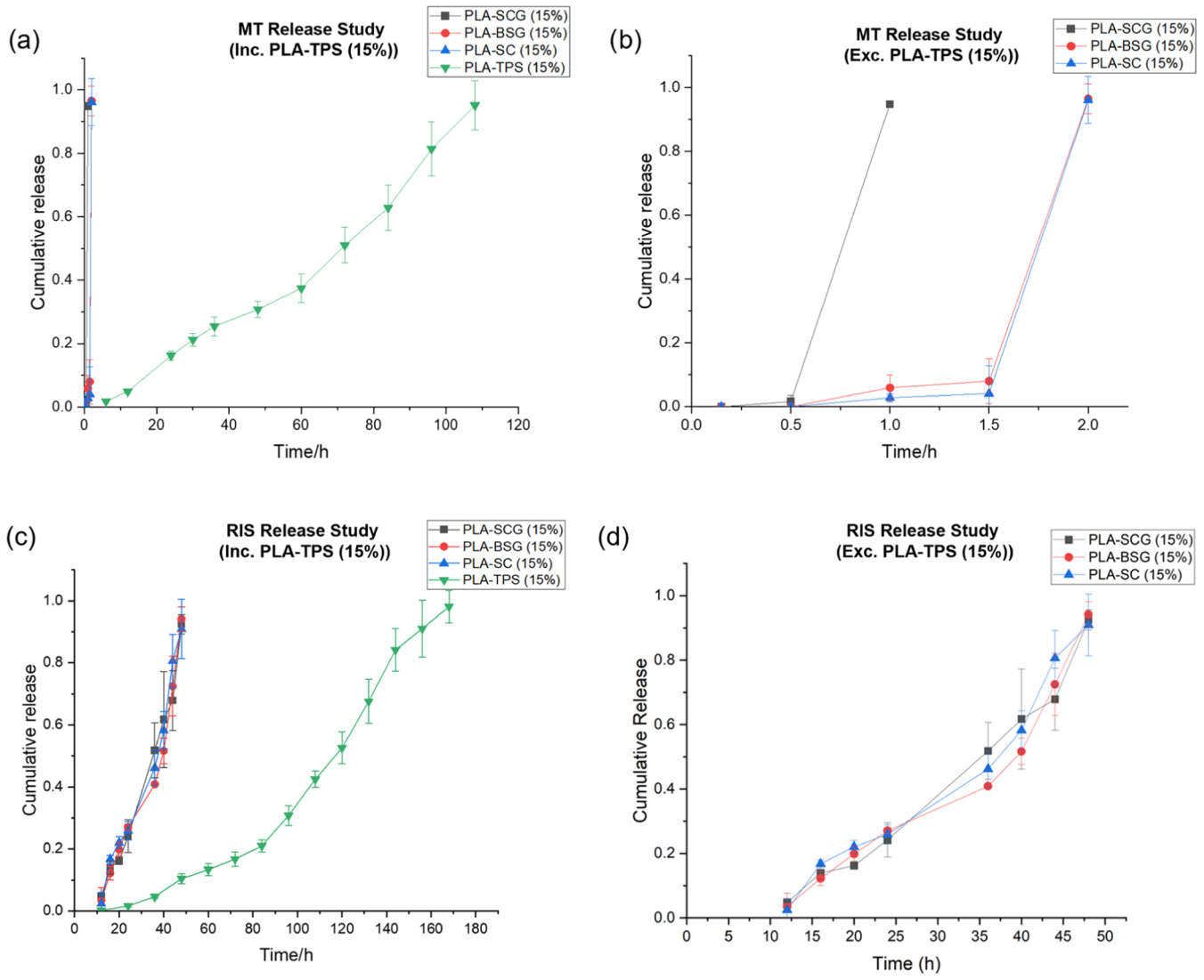

Figure 6. (a) MT release curves of 3DP GFDDS PLA-SC (15%), PLA-BSG (15%), and PLA-SCG (15%), along with PLA-TPS (15%), (b) MT release curves of PLA-food waste only, (c) RIS release curves of 3DP GFDDS PLA-SC (15%), PLA-BSG (15%), and PLA-SCG (15%), along with PLA-TPS (15%), and (d) RIS release curves of PLA-food waste only.

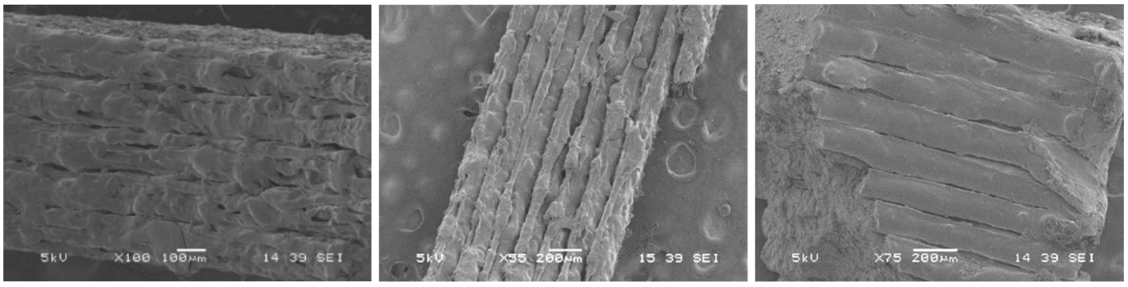

Figure 7. (From left to right) SEM images of 3DP GFDDPS capsules for PLA-SC (15%), PLA-BSG (15%), and PLA-SCG (15%).

manipulated by changing the wall thickness and TPS weight ratio in the 3DP GFDDS capsule. In PLA-food wastes, MT had a delayed burst release profile between 0.5 and 2 h, and RIS was found to have sustained release up to 48 h. While the sustained release profile does not extend as long as PLA-TPS, a delayed release and a 48 h release can still find applications for specific drugs. This is an important milestone, as this approach has yet to be explored. Furthermore, the potential of PLA-food waste composites lies in their ability to tailor drug release profiles while concurrently addressing environmental concerns by repurposing food waste. The work provides the first study that has considered the use of such a PLA composite with TPS and food wastes to adjust the rate of drug release. Furthermore, the incorporation of food waste as a composite offers a sustainable system that is economical in scale. While the byproducts are of similar composition to edible food (for example, sesame seed from SC, and grains from BSG), studies on the safety of these food byproducts warrant further

https://doi.org/10.1021/acsomega.4c05155
ACS Omega 2024, 9, 34140−34150

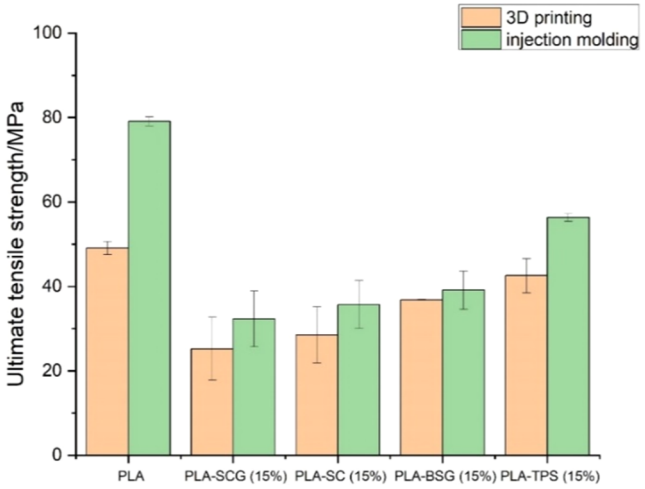

Figure 8. Ultimate tensile strength of samples made by 3D printing and injection molding of PLA, PLA-SC (15%), PLA-BSG (15%), PLA-SCG (15%), and PLA-TPS (15%).

investigation. Alternatively, the use of such a delivery system on other nonedible applications may be advantageous in the controlled release of bioactive.

■ ASSOCIATED CONTENT

Supporting Information

The Supporting Information is available free of charge at https://pubs.acs.org/doi/10.1021/acsomega.4c05155.

Mechanical test results of PLA and PLA-TPS injection molding samples; melting and decomposition temperature of the PLA-TPS composites, DSC thermograms of PLA,TPS, PLA-TPS in various ratios, food waste, and PLA-food waste (15%); TGA thermogram of PLA, and PLA-TPS in various ratios; mass loss of PLA-TPS (40, 50, 60%) samples after putting in SGF 7 and 14 days (PDF)

■ AUTHOR INFORMATION

Corresponding Author

Say Chye Joachim Loo − *School of Materials Science and Engineering, Nanyang Technological University, 639798, Singapore; Lee Kong Chian School of Medicine, Nanyang Technological University, 636921, Singapore; Singapore Centre for Environmental Life Sciences Engineering, Nanyang Technological University, 637551, Singapore;* orcid.org/0000-0001-5300-1275; Email: joachimloo@ntu.edu.sg

Authors

Liwen Wang − *School of Materials Science and Engineering, Nanyang Technological University, 639798, Singapore*

Ling Xin Yong − *School of Materials Science and Engineering, Nanyang Technological University, 639798, Singapore; Singapore Centre for Environmental Life Sciences Engineering, Nanyang Technological University, 637551, Singapore*

Complete contact information is available at: https://pubs.acs.org/10.1021/acsomega.4c05155

Author Contributions

‖L.W. and L.X.Y. contributed equally to this work.

Notes

The authors declare no competing financial interest.

■ ACKNOWLEDGMENTS

Our sincere appreciation towards Starbucks Coffee Singapore Pte Ltd, Oh Chin Hing Sesame Oil Factory, and Par International Pte Ltd for providing the food waste used in this study. We would like to extend our sincere gratitude to the Singapore Centre for 3D Printing (SC3DP) for allowing us to use the Noztek Pro single extruder filament extruder. L.W. acknowledges the Ministry of Education, Singapore (MOE) for the provision of her tuition grant for her Master of Engineering (Research) in the School of Materials Science and Engineering course at Nanyang Technological University. This work was supported by the Singapore Food Agency (SFS_RND_SUFP_001_06) and the Ministry of Education (RG79/22).

■ REFERENCES

(1) Hagen, R. Polylactic Acid. In *Polymer Science: A Comprehensive Reference*; Elsevier, 2012; pp 231−236.
(2) Ebrahimi, F.; Ramezani Dana, H. Poly lactic acid (PLA) polymers: from properties to biomedical applications. *Int. J. Polym. Mater. Polym. Biomater.* **2022**, *71*, 1117−1130.
(3) Alsaheb, R. A. A.; Aladdin, A.; Zalina, N.; et al. Recent applications of polylactic acid in pharmaceutical and medical industries. *J. Chem. Pharm. Res.* **2015**, *7* (51), 51−63.
(4) Auras, R.; Harte, B.; Selke, S. An Overview of Polylactides as Packaging Materials. *Macromol. Biosci.* **2004**, *4*, 835−864.
(5) Decode the Future of Polylactic Acid, 2023. chemanalyst.comhttps://www.chemanalyst.com/industry-report/polylactic-acid-pla-market-673.
(6) Xiao, L.; Wang, B.; Yang, G.; Gauthier, M. Poly(Lactic Acid)-Based Biomaterials: Synthesis, Modification and Applications. In *Biomedical Science, Engineering and Technology*; InTech, 2012.
(7) *Utilization of By-Products and Treatment of Waste in the Food Industry*; Oreopoulou, V.; Russ, W., Eds.; Springer US, 2007.
(8) Filgueira, D.; Holmen, S.; Melbø, J. K.; et al. Enzymatic-Assisted Modification of Thermomechanical Pulp Fibers To Improve the Interfacial Adhesion with Poly(lactic acid) for 3D Printing. *ACS Sustainable Chem. Eng.* **2017**, *5*, 9338−9346.
(9) Song, X.; He, W.; Yang, S.; Huang, G.; Yang, T. Fused Deposition Modeling of Poly (Lactic Acid)/Walnut Shell Biocomposite Filaments—Surface Treatment and Properties. *Appl. Sci.* **2019**, *9*, No. 4892.
(10) Xu, L.; Crawford, K.; Gorman, C. B. Effects of Temperature and pH on the Degradation of Poly(lactic acid) Brushes. *Macromolecules* **2011**, *44*, 4777−4782.
(11) Ruggero, F.; Gori, R.; Lubello, C. Methodologies to assess biodegradation of bioplastics during aerobic composting and anaerobic digestion: A review. *Waste Manage. Res.* **2019**, *37*, 959−975.
(12) da Silva, D.; Kaduri, M.; Poley, M.; et al. Biocompatibility, biodegradation and excretion of polylactic acid (PLA) in medical implants and theranostic systems. *Chem. Eng. J.* **2018**, *340*, 9−14.
(13) Bakan, J. A. Microcapsule Drug Delivery Systems. In *Polymers in Medicine and Surgery*; Springer US: Boston, MA, 1975; pp 213−235.
(14) Bala, R.; Khanna, S.; Pawar, P.; Arora, S. Orally dissolving strips: A new approach to oral drug delivery system. *Int. J. Pharm. Invest.* **2013**, *3*, No. 67.
(15) Koutsamanis, I.; Roblegg, E.; Spoerk, M. Controlled delivery via hot-melt extrusion: A focus on non-biodegradable carriers for non-oral applications. *J. Drug Delivery Sci. Technol.* **2023**, *81*, No. 104289.
(16) Repka, M. A.; Majumdar, S.; Battu, S. K.; Srirangam, R.; Upadhye, S. B. Applications of hot-melt extrusion for drug delivery. *Expert Opin. Drug Delivery* **2008**, *5*, 1357−1376.

(17) Patil, H.; Tiwari, R. V.; Repka, M. A. Hot-Melt Extrusion: from Theory to Application in Pharmaceutical Formulation. *AAPS PharmSciTech* **2016**, *17*, 20−42.
(18) Bácskay, I.; Ujhelyi, Z.; Fehér, P.; Arany, P. The Evolution of the 3D-Printed Drug Delivery Systems: A Review. *Pharmaceutics* **2022**, *14*, No. 1312.
(19) Fan, D.; Li, Y.; Wang, X.; et al. Progressive 3D Printing Technology and Its Application in Medical Materials. *Front. Pharmacol.* **2020**, *11*, No. 122.
(20) Beg, S.; Almalki, W. H.; Malik, A.; et al. 3D printing for drug delivery and biomedical applications. *Drug Discovery Today* **2020**, *25*, 1668−1681.
(21) Sanchez-Rexach, E.; Johnston, T. G.; Jehanno, C.; Sardon, H.; Nelson, A. Sustainable Materials and Chemical Processes for Additive Manufacturing. *Chem. Mater.* **2020**, *32*, 7105−7119.
(22) Hossain, N.; Chowdhury, M. A.; Shuvho, M. B. A.; Kashem, M. A.; Kchaou, M. 3D-Printed Objects for Multipurpose Applications. *J. Mater. Eng. Perform.* **2021**, *30*, 4756−4767.
(23) Ngo, T. D.; Kashani, A.; Imbalzano, G.; Nguyen, K. T. Q.; Hui, D. Additive manufacturing (3D printing): A review of materials, methods, applications and challenges. *Composites, Part B* **2018**, *143*, 172−196.
(24) Gibson, I.; Rosen, D.; Stucker, B. *Additive Manufacturing Technologies: 3D Printing, Rapid Prototyping, and Direct Digital Manufacturing*, 2nd ed.; Springer, 2015.
(25) Ren, Z.; Zhou, X.; Ding, K.; et al. Design of sustainable 3D printable polylactic acid composites with high lignin content. *Int. J. Biol. Macromol.* **2023**, *253*, No. 127264.
(26) Muthe, L. P.; Pickering, K.; Gauss, C. A Review of 3D/4D Printing of Poly-Lactic Acid Composites with Bio-Derived Reinforcements. *Compos., Part C: Open Access* **2022**, *8*, No. 100271.
(27) Alqahtani, A. A.; Mohammed, A. A.; Fatima, F.; Ahmed, M. M. Fused Deposition Modelling 3D-Printed Gastro-Retentive Floating Device for Propranolol Hcl Tablets. *Polymers* **2023**, *15*, No. 3554.
(28) Mora-Castaño, G.; Millán-Jiménez, M.; Caraballo, I. Hydrophilic High Drug-Loaded 3D Printed Gastroretentive System with Robust Release Kinetics. *Pharmaceutics* **2023**, *15*, No. 842.
(29) Giri, B.; Song, E.; Kwon, J.; et al. Fabrication of Intragastric Floating, Controlled Release 3D Printed Theophylline Tablets Using Hot-Melt Extrusion and Fused Deposition Modeling. *Pharmaceutics* **2020**, *12*, No. 77.
(30) Haryńska, A.; Janik, H.; Sienkiewicz, M.; Mikolaszek, B.; Kucińska-Lipka, J. PLA−Potato Thermoplastic Starch Filament as a Sustainable Alternative to the Conventional PLA Filament: Processing, Characterization, and FFF 3D Printing. *ACS Sustainable Chem. Eng.* **2021**, *9*, 6923−6938.
(31) Przybytek, A.; Sienkiewicz, M.; Kucińska-Lipka, J.; Janik, H. Preparation and characterization of biodegradable and compostable PLA/TPS/ESO compositions. *Ind. Crops Prod.* **2018**, *122*, 375−383.
(32) Bartos, A.; Kócs, J.; Anggono, J.; Móczó, J.; Pukánszky, B. Effect of fiber attrition, particle characteristics and interfacial adhesion on the properties of PP/sugarcane bagasse fiber composites. *Polym. Test.* **2021**, *98*, No. 107189.
(33) Farcas, A. C.; Socaci, S. A.; Chiş, M. S.; et al. Reintegration of Brewers Spent Grains in the Food Chain: Nutritional, Functional and Sensorial Aspects. *Plants* **2021**, *10*, No. 2504.
(34) Amoriello, T.; Mellara, F.; Galli, V.; Amoriello, M.; Ciccoritti, R. Technological Properties and Consumer Acceptability of Bakery Products Enriched with Brewers' Spent Grains. *Foods* **2020**, *9*, No. 1492.
(35) Wan, Y.; Zhou, Q.; Zhao, M.; Hou, T. Byproducts of Sesame Oil Extraction: Composition, Function, and Comprehensive Utilization. *Foods* **2023**, *12*, No. 2383.
(36) Shi, C.; Chen, Y.; Yu, Z.; et al. Sustainable and superhydrophobic spent coffee ground-derived holocellulose nanofibers foam for continuous oil/water separation. *Sustainable Mater. Technol.* **2021**, *28*, No. e00277.
(37) Tapangnoi, P.; Sae-Oui, P.; Naebpetch, W.; Siriwong, C. Preparation of purified spent coffee ground and its reinforcement in natural rubber composite. *Arabian J. Chem.* **2022**, *15*, No. 103917.
(38) Lynch, K. M.; Steffen, E. J.; Arendt, E. K. Brewers' spent grain: a review with an emphasis on food and health. *J. Inst. Brewing* **2016**, *122*, 553−568.
(39) Frone, A. N.; Berlioz, S.; Chailan, J. F.; Panaitescu, D. M. Morphology and thermal properties of PLA−cellulose nanofibers composites. *Carbohydrate Polymers* **2013**, *91*, 377−384.
(40) Atif, R.; Inam, F. Reasons and remedies for the agglomeration of multilayered graphene and carbon nanotubes in polymers. *Beilstein J. Nanotechnol.* **2016**, *7*, 1174−1196.
(41) Dumpa, N. R.; Bandari, S.; Repka, M. A. Novel Gastroretentive Floating Pulsatile Drug Delivery System Produced via Hot-Melt Extrusion and Fused Deposition Modeling 3D Printing. *Pharmaceutics* **2020**, *12*, No. 52.
(42) Chai, X.; Chai, H.; Wang, X.; et al. Fused deposition modeling (FDM) 3D printed tablets for intragastric floating delivery of domperidone. *Sci. Rep.* **2017**, *7*, No. 2829, DOI: 10.1038/s41598-017-03097-x.
(43) von Windheim, N.; Collinson, D. W.; Lau, T.; Brinson, L. C.; Gall, K. The influence of porosity, crystallinity and interlayer adhesion on the tensile strength of 3D printed polylactic acid (PLA). *Rapid Prototyp J.* **2021**, *27*, 1327−1336.
(44) Vlachopoulos, A.; Karlioti, G.; Balla, E.; et al. Poly(Lactic Acid)-Based Microparticles for Drug Delivery Applications: An Overview of Recent Advances. *Pharmaceutics* **2022**, *14*, No. 359.
(45) da Silva, D.; Kaduri, M.; Poley, M.; et al. Biocompatibility, biodegradation and excretion of polylactic acid (PLA) in medical implants and theranostic systems. *Chem. Eng. J.* **2018**, *340*, 9−14.
(46) Domsta, V.; Hänsch, C.; Lenz, S.; et al. The Influence of Shape Parameters on Unidirectional Drug Release from 3D Printed Implants and Prediction of Release from Implants with Individualized Shapes. *Pharmaceutics* **2023**, *15*, No. 1276.
(47) Thakkar, R.; Pillai, A. R.; Zhang, J.; et al. Novel On-Demand 3-Dimensional (3-D) Printed Tablets Using Fill Density as an Effective Release-Controlling Tool. *Polymers* **2020**, *12*, No. 1872.
(48) Sadia, M.; Arafat, B.; Ahmed, W.; Forbes, R. T.; Alhnan, M. A. Channelled tablets: An innovative approach to accelerating drug release from 3D printed tablets. *J. Controlled Release* **2018**, *269*, 355−363.
(49) Maroni, A.; Melocchi, A.; Parietti, F.; et al. 3D printed multi-compartment capsular devices for two-pulse oral drug delivery. *J. Controlled Release* **2017**, *268*, 10−18.
(50) Mazarura, K. R.; Kumar, P.; Choonara, Y. E. Customized 3D printed multi-drug systems: an effective and efficient approach to polypharmacy. *Expert Opin. Drug Delivery* **2022**, *19*, 1149−1163.
(51) Robles-Martinez, P.; Xu, X.; Trenfield, S. J.; et al. 3D Printing of a Multi-Layered Polypill Containing Six Drugs Using a Novel Stereolithographic Method. *Pharmaceutics* **2019**, *11*, No. 274.
(52) Khaled, S. A.; Burley, J. C.; Alexander, M. R.; Yang, J.; Roberts, C. J. 3D printing of tablets containing multiple drugs with defined release profiles. *Int. J. Pharm.* **2015**, *494*, 643−650.
(53) García-Domínguez, A.; Claver, J.; Camacho, A. M.; Sebastián, M. A. Considerations on the Applicability of Test Methods for Mechanical Characterization of Materials Manufactured by FDM. *Materials* **2020**, *13*, No. 28.

https://doi.org/10.1021/acsomega.4c05155
ACS Omega 2024, 9, 34140−34150